

## Effect of compensation and of metallic impurities on the electrical properties of Cz-grown solar grade silicon

Joris Libal,<sup>1,a)</sup> Sara Novaglia,<sup>1</sup> Maurizio Acciarri,<sup>1</sup> Simona Binetti,<sup>1</sup> Roman Petres,<sup>2</sup> Jayaprasad Arumughan,<sup>2</sup> Radovan Kopecek,<sup>2</sup> and Aleksander Prokopenko<sup>3</sup>

<sup>1</sup>*Dipartimento di Scienza dei Materiali, Università degli Studi Milano-Bicocca, via Cozzi 53, I-20125 Milano, Italy*

<sup>2</sup>*ISC -Konstanz, Rudolf-Diesel-Str. 15, D-78467 Konstanz, Germany*

<sup>3</sup>*Joint-Stock Company Pillar (JSC Pillar), Severo-Syretska str. 3, Kiev 04136, Ukraine*

(Received 18 April 2008; accepted 4 October 2008; published online 20 November 2008)

In this work we present a study of a *p*-type Czochralski-grown Si ingot which was grown using 10% solar grade silicon (SoG-Si). As the SoG-Si contains a relatively high concentration of impurities including phosphorus, the electrical properties of the as-grown wafers from this ingot are affected by both the compensating dopants and other impurities. Measurements of the minority charge carrier lifetime in the as-grown material reveal very low values (4–8  $\mu$ s). The Hall mobilities at room temperature correspond to normal values for Czochralski silicon in the upper part of the ingot (which solidifies first) and decrease significantly toward the bottom of the ingot. Segregation leads to an accumulation of impurities toward the lower parts of the ingot as well as to a stronger increase in phosphorus than of boron, the latter of which results in a high compensation level (i.e., an increasing resistivity). A priori, both effects could be responsible for the degradation of the electrical properties in the lower parts of the ingot, whereas theoretical considerations show that the level of compensation should not cause a strong decrease in Hall mobility at room temperature. Untextured solar cells have been processed from wafers originating from different positions of the ingot. As expected, the phosphorus diffusion leads to a gettering effect: the recombination active impurities are removed out of the wafer volume. This results in relatively high efficiencies (>16%) of the solar cells but does not show a strong correlation between ingot height and cell efficiency. This observation is also confirmed by the high bulk lifetimes (>200  $\mu$ s) measured after the process even for samples originating from the last solidified (lower) part of the ingot. The Hall mobility of samples cut from finished solar cells has been measured and shows the same trend as the as-grown samples, the values for the bottom of the ingot still being very low. With the concentrations of boron and phosphorus studied up to this point, compensation showed no detrimental effect on the cell efficiency of industrial-like solar cells. © 2008 American Institute of Physics.

[DOI: [10.1063/1.3021300](https://doi.org/10.1063/1.3021300)]

### INTRODUCTION

The actual silicon production capacities do not keep up with the sustained high growth rate of the photovoltaic (PV) industry. As the PV industry is expected to remain based mostly on crystalline silicon at least for the next decade, a substantial increase in the amount of Si produced is needed both in order to enable this growth and to decrease the cost of Si feedstock and thus the cost per  $W_{\text{peak}}$  of PV generated electricity. For this aim—in addition to the construction of plants using the traditional Siemens purification process—efforts are made in order to develop less energy consuming processes for the purification of metallurgical-grade Si (e.g., Refs. 1 and 2). In comparison to the Siemens process, which has been developed according to the strict requirements of the microelectronic industry, these processes result in less pure Si: so-called solar grade silicon (SoG-Si). The main aim of research in this field is the determination of the maximum concentrations of impurities that can be tolerated in the SoG-Si feedstock without an excessive loss in efficiency of

the resulting solar cells. Besides a variety of metallic impurities (Fe, Mo, Ti, etc.), SoG-Si generated by such alternative refining processes often contains a large amount of the doping elements boron and phosphorus. These require particular attention for two reasons: first, because of their relatively high segregation coefficients ( $k_B=0.8$ ,  $k_P=0.35$ ), they are not easily removable by segregation, e.g., during the solidification of a multicrystalline or monocrystalline ingot and second their presence changes the concentrations of free charge carriers and consequently the specific resistivity of the Si material. If the specific resistivity is not within a suitable range, it can have a strong negative impact on solar cell efficiency. Thus, when studying SoG-Si, besides determining the maximum concentrations of different (metallic) impurities, it is also important to determine the maximum concentrations of the doping elements that are acceptable. Thereby, the effect of the simultaneous presence of B and P, i.e., compensation, has to be taken into account.

The compensation of *p*-type Si with phosphorus for PV applications has already been studied experimentally in the last decades.<sup>3–5</sup> The compensation levels of the Si samples studied in these former works are presented together with the

<sup>a)</sup>Electronic mail: [joris.libal@unimib.it](mailto:joris.libal@unimib.it)

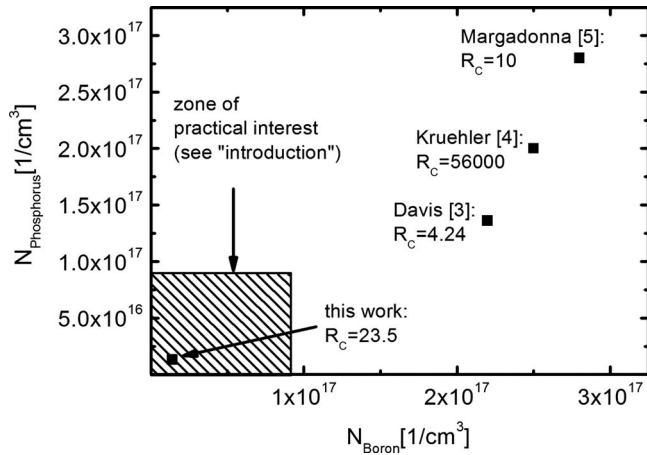


FIG. 1. Donor and acceptor concentrations and compensation ratio  $R_c$  of the material studied in this work in comparison with values found in literature.

data of this work in Fig. 1. At the considered levels of compensation, no impact on cell efficiencies or minority carrier diffusion length has been shown. One has to be aware that—except for high-efficiency cell concepts—in the case of monocrystalline silicon, cell efficiencies are generally limited rather by the cell concept than by the diffusion length of the minority charge carriers. That means it has to be taken into account that the solar cell processes used two decades ago limit the efficiency to lower values than modern cell processes do. Consequently, modern cell processes are more sensitive to an eventual negative effect of both metallic impurities and high concentrations of doping elements. Therefore it is useful to reconsider this question in the light of the more efficient cell processes available today.

When looking for eventual effects of compensation in Si—i.e., simultaneous presence of B and P—one important consideration is the resulting resistivity distribution along the ingot height. Depending on the cell concept, there is a limited range of specific resistivities of the Si substrate which are usable without resulting in an excessive loss in cell efficiency. If at the same time, one limits the amount of Si to be cropped from the top and bottom of the ingot, this consideration delivers a boundary condition that allows us to calculate the maximum concentrations of boron and phosphorus in the melt. Solidification of the silicon leads to a distribution of impurities along the ingot due to segregation according to the Scheil equation,

$$C_x = kC_0(1-x)^{k-1},$$

where  $x$  is the solidified fraction of the ingot,  $C_x$  is the concentration of the impurity at this relative ingot height,  $k$  is the segregation coefficient of the considered impurity, and  $C_0$  is the concentration of the impurity in the melt.

The exact numbers in the following calculations depend on the cell concept, on the cost structure of the used cell process and of the Si purification process, and have thus to be considered as approximate values. The efficiency of a standard industrial front junction cell has been modeled using PC1D (Ref. 6) for various specific resistivities of the Si wafer (Fig. 2). Assuming that 10% of the cost of a PV system containing crystalline Si solar cells is due to the polysilicon

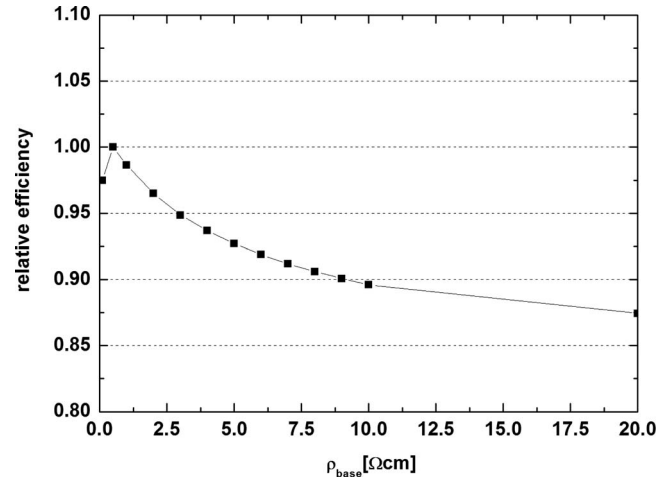


FIG. 2. PC1D simulation of the relative efficiency of a standard industrial front junction solar cell against base resistivity.

feedstock, a relative cell-efficiency loss of 3% would require a cost reduction in SoG-Si with respect to electronic grade (EG)-Si of at least 30% in order to avoid an economic loss. Limiting the relative efficiency loss to values below 3%, the conclusion of this simulation is that the base resistivity should remain between 0.5 and 2  $\Omega$  cm. Limiting the amount of silicon to be cropped to, e.g., 5% from the top of the ingot (material with a resistivity below 0.5  $\Omega$  cm) and to 10% from the bottom of the ingot (resistivity higher than 2  $\Omega$  cm) delivers an additional boundary condition. Under these conditions, the Scheil equation gives peak concentrations of around  $7.7 \times 10^{16} \text{ cm}^{-3}$  for boron and  $7 \times 10^{16} \text{ cm}^{-3}$  for phosphorus at  $x=0.9$ . This implies maximum concentrations of  $4.5 \times 10^{16} \text{ cm}^{-3}$  for phosphorus and  $6.1 \times 10^{16} \text{ cm}^{-3}$  for boron in the melt (and thus, in the used feedstock).

Therefore, in addition to the fact, that very high concentrations (e.g.,  $10^{18} \text{ cm}^{-3}$ ) of boron and phosphorus limit the diffusion length of the minority charge carriers to values below the limit imposed by Auger recombination due to the presence of vacancylike defects,<sup>7</sup> it is not of practical interest to consider these high concentrations for PV applications as they lead to a resistivity distribution in the ingot that causes a high fraction of cropped Si. In the present work we studied the electrical properties of Si samples originating from different heights of a Cz-Si ingot by measuring the lifetime of the minority charge carriers and the mobility (using Hall measurements) of the majority charge carriers. As this ingot was grown using 10%SoG-Si that contained a relatively high concentration of both metallic impurities and phosphorus, segregation resulted in a variation in impurity concentration and compensation level along the ingot height. In order to distinguish the effect of the impurities from the impact of compensation, an industrial solar cell process, which includes phosphorus diffusion gettering, was applied to wafers originating from several heights in the ingot. By this means, samples were obtained with the same compensation level as the as-grown material but with much lower impurity concentrations. In addition to the analysis of the finished solar cells, lifetime, Hall, and secondary ion mass spectroscopy (SIMS) measurements were performed on samples cut from the fin-

ished solar cells. As for the most impurities of interest the detection limit of the SIMS technique is higher than the expected concentrations, these measurements have been conducted in the P-diffused gettering layer. In this way, the nature of the impurities present in the SoG-Si was determined.

## EXPERIMENTAL

The Si ingot used for this study was prepared by the Cz-pulling technique using 90% EG-Si and 10% SoG-Si (total weight of the ingot: 47 kg). The SoG-Si was produced from metallurgical Si by direct carbothermal reduction in ultrapure quartz and carbon black.<sup>8</sup> As the SoG-Si contains a large amount of P (around  $8.5 \times 10^{16} \text{ cm}^{-3}$ ), the resulting melt of EG-Si and SoG-Si received an additional doping with B in order to obtain a target resistivity of around  $2 \Omega \text{ cm}$  in the majority of the ingot. After crystallization, the head and tail of the ingot were removed and the ingot was squared. The ingot was then cut into  $200 \mu\text{m}$  thick,  $156 \times 156 \text{ mm}^2$  semisquare wafers. The numbering of the wafers in the following will be such as that the low numbers denominate wafers originating from the part of the ingot that solidified first (top), whereas the high numbers are assigned to wafers from the part of the ingot that solidified last (bottom).

The resistivity was determined at various positions along the ingot height using the four-point-probe technique. The concentrations of interstitial oxygen ( $O_i$ ) (ASTM F1188-88) and substitutional carbon ( $C_s$ ) (ASTM F1391-93) were determined by fourier-transform infrared (FTIR) spectroscopy measurements. Before measuring the lifetime using the quasi-steady-state photoconductance (QSSPC) technique<sup>9</sup> the as-grown samples were subjected to a polishing etch containing  $\text{HNO}_3$ , HF, and  $\text{CH}_3\text{COOH}$  (removal of  $20 \mu\text{m}$  from each side of the wafer) and a subsequent surface clean by “piranha” solution ( $\text{H}_2\text{O}_2:\text{H}_2\text{SO}_4=1:4$ ) followed by a HF dip. The surface was passivated using an iodine/ethanol solution.<sup>10</sup> The  $\mu$ -wave detected photoconductance decay technique was used to perform laterally resolved lifetime measurements.

In order to prepare the  $1 \times 1 \text{ cm}^2$  samples for measurement of the Hall mobility, a thermally evaporated aluminum layer was deposited on small areas in the four corners of the samples according to the van der Pauw geometry and the samples were then annealed at  $450 \text{ }^\circ\text{C}$  for 15 min. In order to perform the mobility measurements in a temperature range from 80 to 300 K, the samples have been mounted in a closed cycle helium cryostat. The maximum of the magnetic field was  $B=0.5 \text{ T}$ . Solar cells have been processed using a standard industrial-like process consisting of saw damage removal by hot NaOH, P diffusion ( $\text{POCl}_3$  in an open-tube furnace), plasma-enhanced chemical-vapor deposition  $\text{SiN}_x$  coating of the front surface, screen printing of the front (Ag paste) and the rear contacts (Al paste), and cofiring of the contacts in a metal belt furnace. No surface texture has been applied. At the end of the process, the  $p/n$ -junction has been isolated by cutting with a dicing saw and the illuminated  $I/V$  characteristics of the solar cells have been measured under standard conditions (1 sun, AM1.5,  $25 \text{ }^\circ\text{C}$ ). For lifetime and

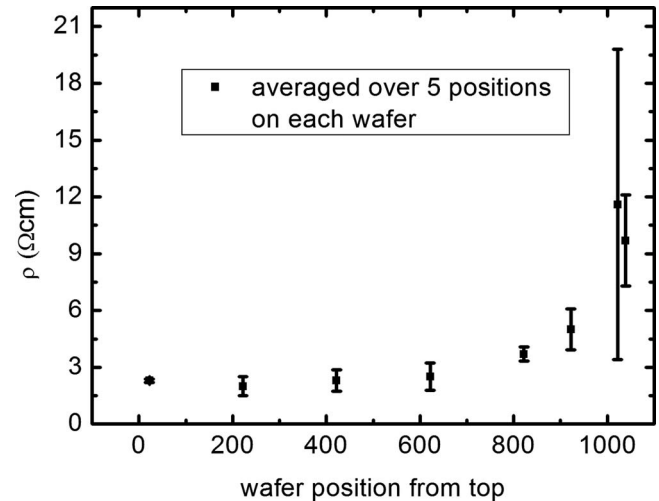


FIG. 3. Distribution of the resistivity along the ingot height—measured using the four-point-probe technique.

Hall measurements, samples have been cut from the solar cells and the metal contacts and doped regions have been removed. The SIMS measurements have been performed on samples cut from the solar cells without any pretreatment in order to measure the concentrations of the impurities accumulated in P-gettered regions.

## RESULTS AND DISCUSSION

The resistivity profile shows the compensating effect of the P which—due to the different segregation coefficients of boron and phosphorus—leads to an increasing resistivity toward higher wafer numbers (last solidified part or bottom of the ingot) (Fig. 3). The  $C_s$  shows a significant increase toward higher wafer numbers according to its small segregation coefficient ( $k_C=0.05$ ). In contrast to that, the  $O_i$  shows no significant trend and is at a level that is usual for Cz-Si: around  $1 \times 10^{18} \text{ atoms/cm}^3$  (Fig. 4).

The mobility  $\mu_H$  of the majority charge carriers at room temperature, determined by Hall measurements (Fig. 5), shows a strong decrease in  $\mu_H$  toward the bottom of the ingot. The temperature dependent carrier concentrations  $p(T)$  have been determined on samples originating from different positions of the ingot by Hall measurements at temperatures

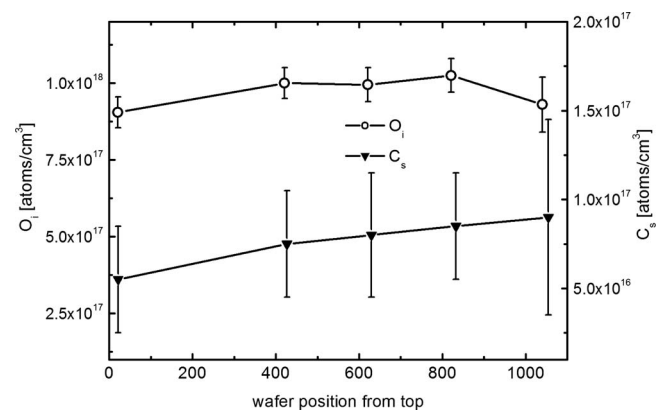


FIG. 4. Concentration of interstitial oxygen and substitutional carbon concentration vs ingot height (determined by FTIR).

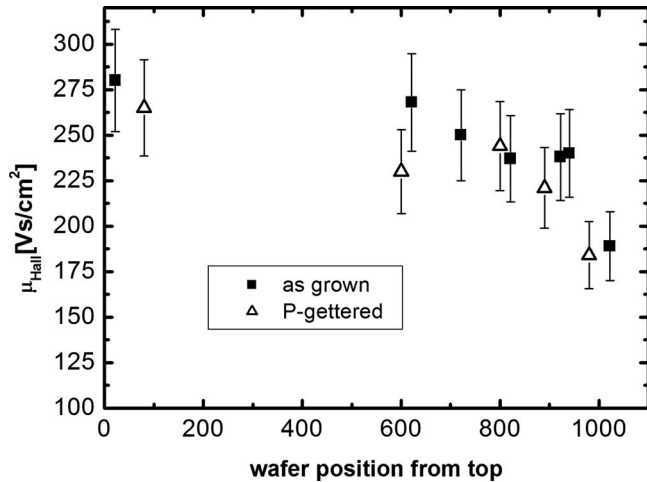


FIG. 5. Hall measurements at room temperature on as-grown samples in comparison to the values obtained on samples cut from finished solar cells.

between 80 and 300 K (one example is shown in Fig. 6). From these data, the concentration of acceptors  $N_a$  and donors  $N_d$  in the material can be calculated by fitting the experimental data  $p(T)$  to the charge balance equation,<sup>11</sup>

$$\frac{p(p + N_d)}{(N_a - N_d - p)} = \frac{1}{\beta} N_v \exp\left(\frac{E_a}{kT}\right),$$

where  $E_a = E_c - E_d$  is the donor ionization energy,  $\beta$  is the spin degeneration factor,  $N_v$  is the density of states in the valence band, and  $k$  is the Boltzmann constant.

The values for the carrier concentrations  $p(T)$  are obtained by the well known relation  $p(T) = r_H / eR_H$ , where  $r_H$  is the Hall factor,  $e$  is the electron charge, and  $R_H$  is the measured Hall coefficient. As a first approximation, we made the assumption that  $r_H = 1$  although we know that this value is valid only in presence of high magnetic field. We will come back to this approximation later in the paper. The calculated concentrations of donors and acceptors and the corresponding compensation ratios  $R_c = (N_a + N_d) / (N_a - N_d)$  are shown in Figs. 7 and 8.

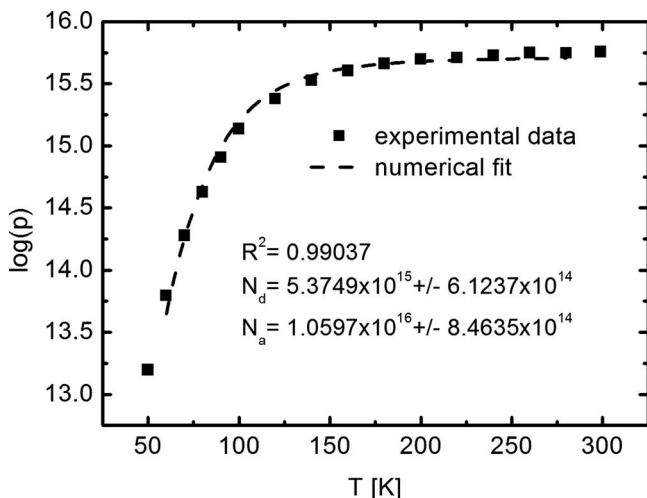


FIG. 6. Numerical fit to the temperature dependent carrier concentration (from Hall measurement) for determination of the donor and acceptor concentrations (wafer from position 821).

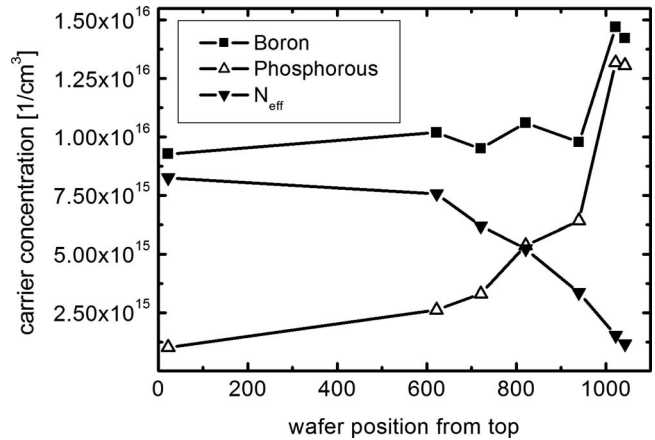


FIG. 7. Donor and acceptor concentrations and  $N_{eff}$  along the ingot, calculated from the numerical fits to temperature dependent Hall measurements (see Fig. 6).

QSSPC measurements of the minority charge carrier lifetime have been performed on as-grown samples originating from different ingot heights (Fig. 9). The lifetime at the top of the ingot is around 8  $\mu\text{s}$  and decreases to 4  $\mu\text{s}$  at the bottom of the ingot (at an excess carrier density of  $\Delta n = 1 \times 10^{15} \text{ cm}^{-3}$ ), showing thus the same trend as  $\mu_H$  at room temperature. Considering the fact that the material has been grown using the Cz-pulling technique, these lifetimes are low.

In order to exclude crystal defects as a possible reason for the low electrical quality of the material, a defect etch (Sopori) has been performed on samples originating from the bottom, middle, and top of the ingot and the etch pit density (EPD) has been evaluated. As expected for Cz-Si material grown according to the state of the art, the defect density in all samples is very low: they range from  $1.5 \times 10^3$  to  $3 \times 10^4 \text{ cm}^{-2}$ .

The segregation coefficient of most metallic impurities is very low [e.g.,  $k_{Fe} = 6.4 \times 10^{-6}$  (Ref. 3)], causing a strong accumulation of these elements (introduced by the 10% of SoG-Si) toward the bottom of the ingot. Consequently, two

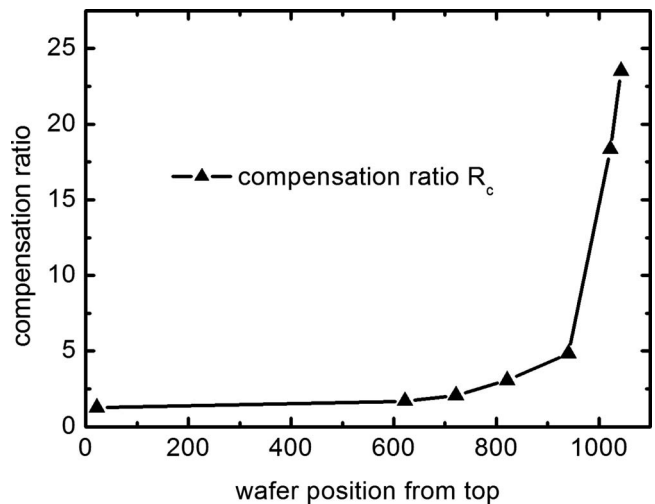


FIG. 8. Compensation ratio  $R_c = (N_a + N_d) / (N_a - N_d)$  along the ingot height—calculated from data in Fig. 7.

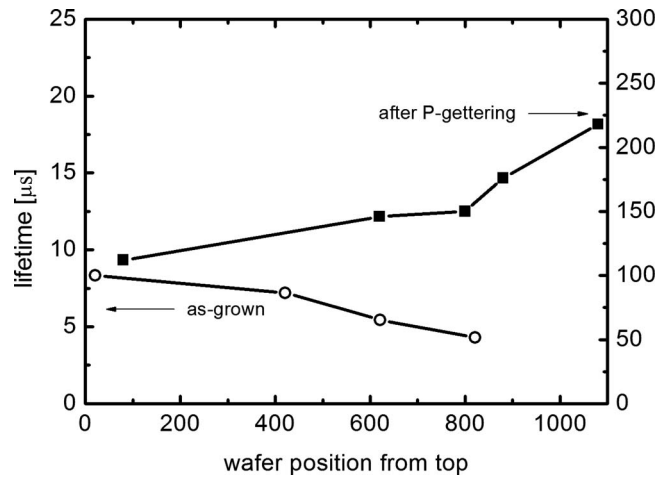


FIG. 9. Lifetime measured on  $5 \times 5 \text{ cm}^2$  samples as grown and after the solar cell process (determined with QSSPC at an excess carrier density of  $\Delta n = 2.5 \times 10^{15} \text{ 1/cm}^3$ ).

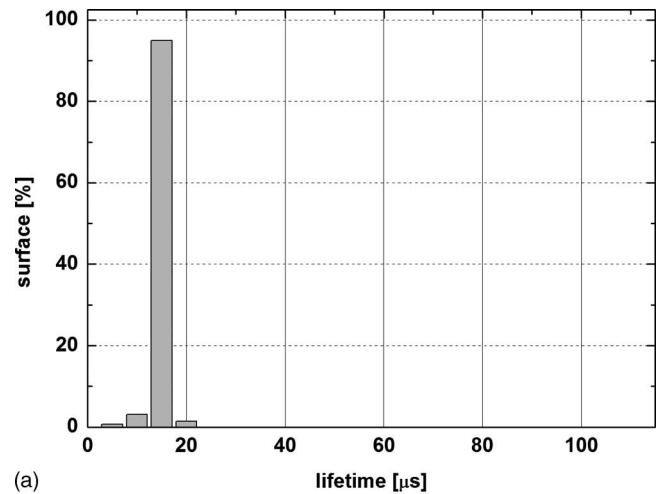
possible reasons for the low minority charge carrier lifetime and the low mobility of the majority carriers in the bottom part of the ingot are the increasing compensation by phosphorus on the one hand and the strong accumulation of metallic impurities on the other hand.

### SOLAR CELLS AND MATERIAL PROPERTIES AFTER SOLAR PROCESSING

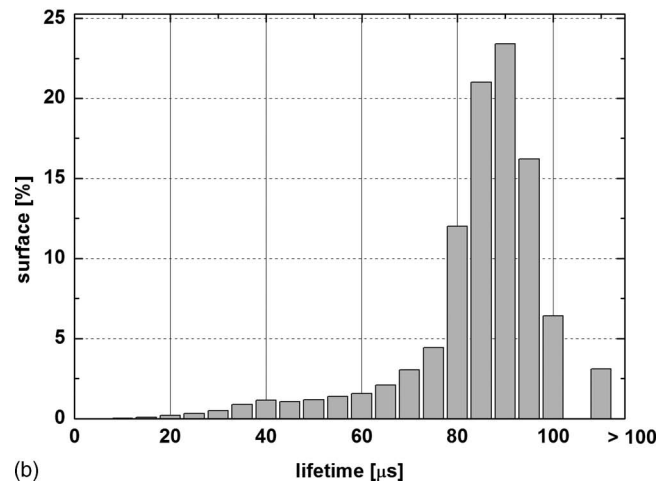
High temperature steps occurring during solar cell processing—particularly the gettering effect of the P diffusion—are known to change the electrical properties of Si wafers. As the efficiency of solar cells is determined by the material properties after cell processing, measurements on samples cut from finished solar cells will be presented in the following. The cells have been fabricated applying the process described above.

After removal of the metal contacts and the diffused regions (emitter and back-surface field), QSSPC lifetime measurements have been performed on  $5 \times 5 \text{ cm}^2$  sections cut from finished solar cells. In order to minimize recombination at B–O complexes, these samples have been submitted to a heat treatment under illumination (2 h at  $150 \text{ }^\circ\text{C}$  on a hot-plate, 400 W halogen lamp). According in Ref. 12, this kind of treatment transforms the B–O complexes into a stable nonrecombinant state and thus avoids instable lifetime values due to light-induced degradation (LID). The results of lifetime measurements (after deactivation of the B–O complexes) of the P-gettered samples are shown in Fig. 9 and show a significant increase in the minority charge carrier lifetime with respect to the as-grown values due to the well known impurity gettering effect of the P diffusion. In addition, the lifetime increases with decreasing majority carrier density  $N_{\text{eff}}$ .

Lifetime mappings have been performed using the  $\mu$ -wave photoconductance-decay ( $\mu$ W-PCD) technique on two neighboring  $15.6 \times 15.6 \text{ cm}^2$  wafers—one as grown and the other after P gettering. The associated histograms demonstrate the good lateral homogeneity of the lifetime increase [Figs. 10(a) and 10(b)]. In order to determine the nature of



(a)



(b)

FIG. 10. Histograms from  $\mu$ W-PCD lifetime mappings of (a) as-grown and (b) P-gettered wafers from ingot position 430.

the gettered impurities, SIMS measurements have been performed in the P-diffused region (emitter) of samples cut from the finished solar cells. Two examples are shown in Fig. 11. Looking at the absolute values for the concentrations, the following remarks should be taken into account: Al, Ca, Cr, Fe, Ni, and Cu were calibrated using implanted reference samples, while Ti and Mo have been determined using relative sensitivity factors (and should thus be considered only as indicative). Additionally, although a high mass resolution has been used in order to reduce the potential influence of interfering ions/molecules in the mass separation, this mass separation may not be perfect. In particular, it is not possible to separate the isotopes  $^{54}\text{Fe}$  (this isotope for Fe has been used because  $^{56}\text{Fe}$  interferes with  $^{28}\text{Si}_2$ ) and  $^{54}\text{Cr}$ ; thus the profile of Fe will contain a contribution from Cr. Further, as no reference for Ti has been available, it is difficult to distinguish between  $^{48}\text{Ti}$  and  $^{16}\text{O}_3$ .

The qualitative conclusion of the SIMS measurements is that Al, Ca, Fe, Cu, and Ti are the most important impurities that are gettered and that are accordingly present in the SoG-Si [Figs. 11(a) and 11(b)]. In addition to that, Mo, Ni, and Cr have been detected [Figs. 11(c) and 11(d)].

The P gettering reduces the concentration of metallic impurities but leaves the donor and acceptor concentration un-

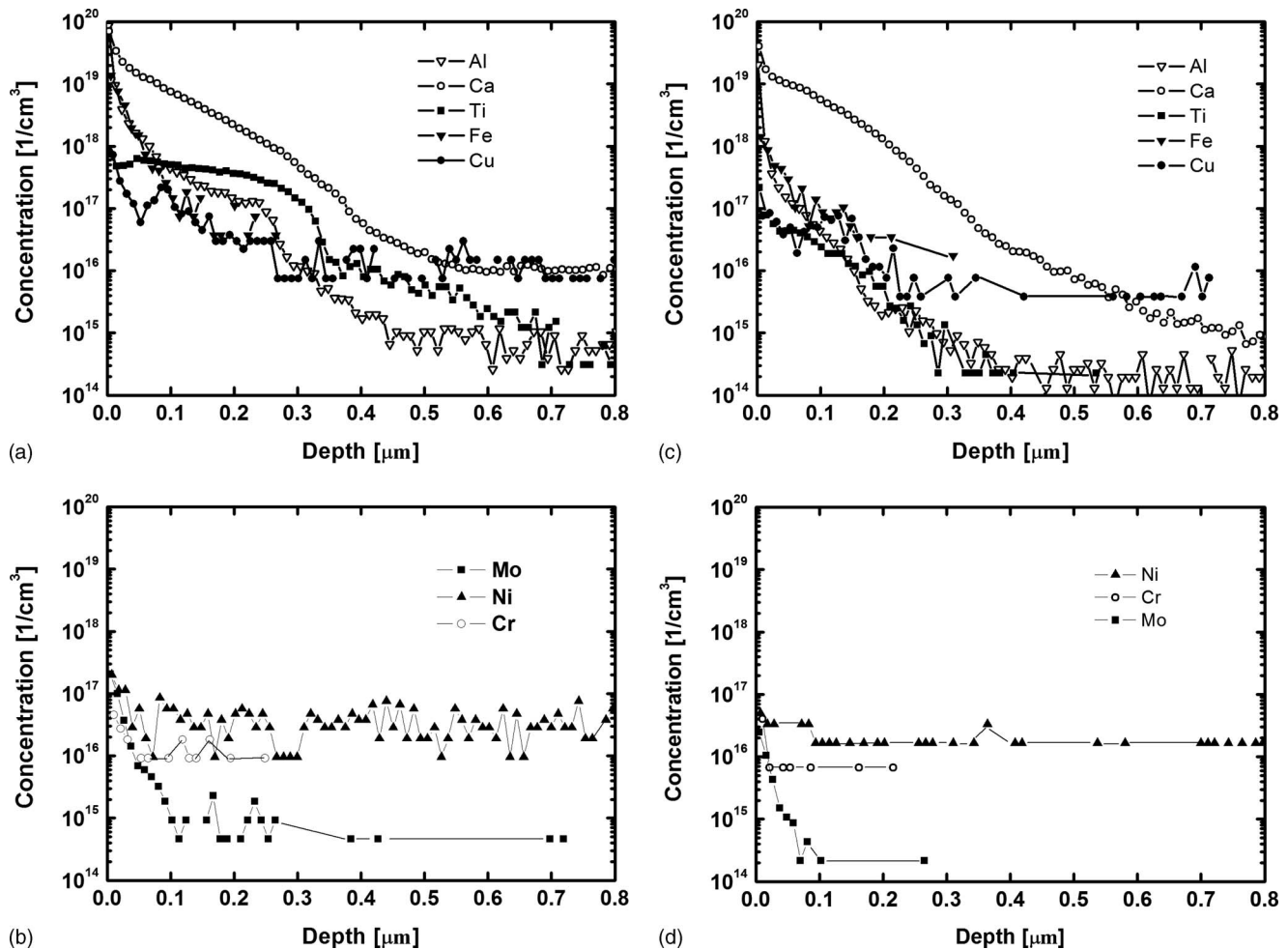


FIG. 11. [(a) and (b)] SIMS of P-gettered region (position 620); [(c) and (d)] SIMS of P-gettered region (position 1040).

changed. Consequently, the study of samples cut from solar cells enables a separation of the impact of impurities from that of compensation.

To study a possible effect of the reduced concentration of metallic impurities on the mobility of the majority charge carriers,  $1 \times 1 \text{ cm}^2$  samples have been cut from the processed solar cells and Hall measurements at room temperature have been performed on these samples coming from different heights of the ingot (Fig. 5). The error bars reported here correspond to the systematic error due to the contact geometry using the van der Pauw sample geometry. With respect to this error, no change in  $\mu_H$  at room temperature due to reduction in the impurity concentrations is observed. Hence it seems that the increasing compensation due to the increase in the P concentration toward the bottom of the ingot is responsible for the reduction in  $\mu_H$ .

In order to check this hypothesis a numerical simulation has been performed, taking into account scattering on optical phonons<sup>13</sup> on ionized<sup>14</sup> and neutral impurities<sup>15</sup> as well as the application of Mathiesen's rule.<sup>16</sup> In Fig. 12 the results of this simulation are shown together with the experimental results. Due to  $\mu_{\text{drift}} = r_H \mu_H$  and as the simulated mobility is the drift mobility the experimental values should be multiplied by the Hall factor—which may be influenced by the compensation level. Thus, experimental and calculated values are

normalized to the respective mobility of the sample with the lowest compensation ratio (ingot position 22). The simulation resulted in  $\mu_{\text{drift}} = 487 \text{ cm}^2/\text{V s}$  for position 22 which would result in a Hall factor  $r_H$  of 0.74 supposing that the above listed scattering mechanisms correctly describe the studied material. The decrease in  $\mu_H$  with increasing com-

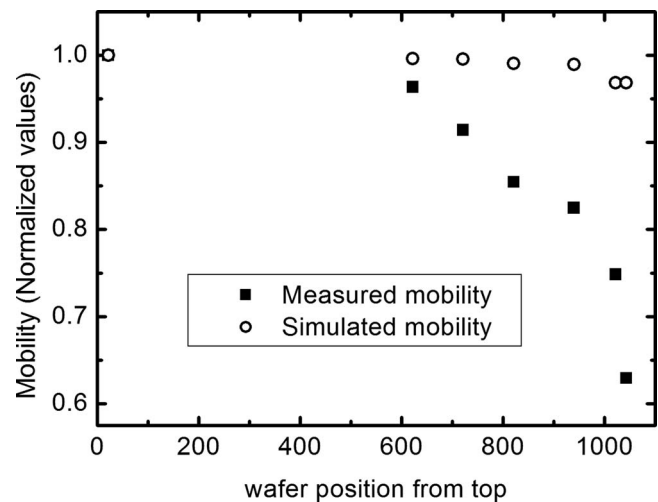


FIG. 12. Comparison of simulated and measured Hall mobilities (at room temperature).

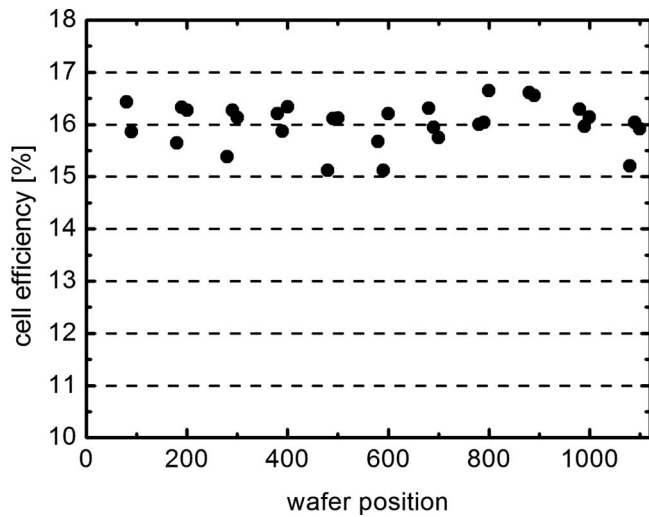


FIG. 13. Efficiency of solar cells fabricated with a standard industrial process (P diffusion,  $\text{SiN}_x$ , screen-printed contacts, and Al-BSF, without surface texture).

compensation could thus be either due to an increased  $r_H$  or due to a reduction in  $\mu_{\text{drift}}$ . According in Ref. 17 increasing  $N_a$  from  $9 \times 10^{15} \text{ cm}^{-3}$  (position 22) to  $1.4 \times 10^{16} \text{ cm}^{-3}$  (position 1040) causes a decrease in  $r_H$  of less than 4%. Calculations from Ref. 18 indicate a decrease in  $r_H$  of less than 5% when increasing  $N_d$  from  $1 \times 10^{15} \text{ cm}^{-3}$  (position 22) to  $1 \times 10^{16} \text{ cm}^{-3}$  (position 1040). This means that the separate consideration of the increase in  $N_a$  and in  $N_d$  cannot explain the fact that  $\mu_H$  in sample 1040 is reduced by 37% (Fig. 12) with respect to the least compensated sample (position 22).

We recall that in the fit for the determination of  $p(T)$  we used  $r_H=1$ . For a more accurate determination of compensation the actual  $r_H$  as a function of doping and temperature should be used. In literature, however, an accepted  $r_H$  value for compensated material as a function of temperature and doping is not reported. Therefore we have to adopt for the mobility the same speculative consideration that we used above for  $p(T)$ .

Looking at the efficiencies of industrial solar cells processed on the studied compensated Cz-Si, the situation is quite different: independent of the wafer position (compensation level) the efficiencies are between 15.1% and 16.7% (Fig. 13). In general, considering a given solar cell concept, the most important material parameter influencing the solar cell efficiency is the diffusion length of the *minority* charge carriers  $L_{\text{diff}}$  which is related to  $\tau_{\text{bulk}}$  by

$$L_{\text{diff}} = \sqrt{D\tau_{\text{bulk}}}$$

with

$$D = \mu_{\text{drift}} \frac{kT}{q},$$

Supposing standard mobility values, the lifetime measured in the most compensated part of the ingot (position 1080,  $\tau_{\text{bulk}}=220 \mu\text{s}$ ) corresponds to  $L_{\text{bulk}} \approx 790 \mu\text{m}$ . Under the (nonconstraining) assumption that the phenomenon observed here has the same impact on the scattering of majority and minority carriers, a reduction in the mobility by 37% would

lead to a reduction in  $L_{\text{bulk}}$  by 20% which is still significantly more than twice the thickness of the wafers. For the industrial cell process applied here, changes in  $L_{\text{bulk}}$  in this range have a very small impact on the cell efficiency and can therefore not be observed in Fig. 13. When applying more sophisticated cell processes with very low surface recombination velocities on the front and rear side of the cell, the variation in  $L_{\text{bulk}}$  could possibly have a measurable influence on the cell efficiency.

## CONCLUSIONS

This study looked at the effects of introducing impurities to a Cz-Si ingot by replacing 10% of the feedstock with SoG-Si. The results show that the impurities can mostly be gettered by a P-diffusion step and are therefore not harmful for the finished solar cell.

On the other hand, a strong reduction in the Hall mobility of the majority charge carriers has been observed in the part of the ingot that was solidified last. As the values for  $\mu_H$  remain unchanged after the removal of metallic impurities during the cell process, the lower mobility values in the part of the ingot that solidified last are attributed to the high compensation ratio in this ingot height. Considering that the cell efficiency is limited by the applied industrial cell process and taking into account the high diffusion lengths of the minority charge carriers after processing, the reduction in  $\mu_H$  has no significant impact on the cell efficiency. Consequently, up to the concentrations of boron and phosphorus studied here, compensation has no detrimental effect on the cell efficiency when applying modern industrially relevant cell processes.

Approaching  $4W_{\text{wafer}}$  ( $W_{\text{wafer}}$ =wafer thickness), the  $L_{\text{bulk}}$  after cell processing is even in a range that would allow the processing of high-efficiency cells using, e.g., the interdigitated back-contact cell concept.<sup>19</sup>

The compensation range obtained with boron and phosphorus concentrations between  $1 \times 10^{16}$  and  $6 \times 10^{17} \text{ cm}^{-3}$  has been shown here to be the interesting range for PV applications and should be studied in future experiments. Another point of practical interest is to study Cz-Si grown from a feedstock containing more than 10% SoG-Si and therefore higher impurity concentrations. The increase in the concentrations of metallic impurities leads to an increased formation of crystal defects<sup>20</sup> which in turn will compromise the gettering efficiency of a P diffusion and thus reduce the final  $L_{\text{bulk}}$ . Consequently the task will consist of determining the maximum concentration of metallic impurities acceptable in the feedstock without an excessive reduction in  $L_{\text{bulk}}$  after the solar cell process. Another phenomenon to be taken into account is the LID due to the formation of B-O complexes. On the one hand, this can be avoided by the use of *n*-type Si (P doping) or possibly, in the case of *p*-type Si, by codoping with phosphorus (compensation).<sup>4</sup> A study of a potential reduction in LID by the formation of nonrecombination active B-P pairs will be subject of a future publication.

Due to the lack of grain boundaries and the much lower density of dislocations, which in multicrystalline (mc) Si tend to retain impurities and impede external gettering, Cz growth may prove to be the better choice when using SoG-Si

as feedstock. Thereby, *n*-type Si could be of particular interest as it shows no LID and as it has proven to be less sensitive to common metallic impurities.<sup>21</sup>

As it has been shown here, an independent consideration of acceptors and donors does not lead to a correct description of the dependence of  $\mu_H$  on  $N_a$  and  $N_d$ . From a theoretical point of view, a model including an interaction between donors and acceptors should be established in order to reproduce numerically the values for  $\mu_H$  in strongly compensated Si presented here.

## ACKNOWLEDGMENTS

This work was supported within the FoXy-project by the European Commission under Contract No. 019811.

- <sup>1</sup>K. Peter, E. Enebakk, K. Friestad, R. Tronstad, and C. Dethloff, Proceedings of the 20th EU PVSECEC, Barcelona, 2005 (unpublished), p. 615.  
<sup>2</sup>N. Yuge, H. Baba, Y. Sakaguchi, K. Nishikawa, H. Terashima, and F. Aratani, *Sol. Energy Mater. Sol. Cells* **34**, 243 (1994).  
<sup>3</sup>J. R. Davis, A. Rohatgi, R. H. Hopkins, P. D. Blais, P. Rai-Choudhury, J. R. McCormick, and H. C. Mollenkopf, *IEEE Trans. Electron Devices* **27**, 4 (1980).  
<sup>4</sup>W. Kruehler, C. Moser, F. W. Schulze, and H. Aulich, Proceedings of the Eighth EU PVSEC, 1988 (unpublished), p. 181.  
<sup>5</sup>D. Margadonna, F. Ferrazza, R. Peruzzi, S. Pizzini, C. Acerboni, L. Tarchini, Wei XiWen, and A. de Lillo, Proceedings of the Tenth EU PVSEC, Lissabon, 1991 (unpublished), p. 678.

- <sup>6</sup>P. Basore and P. D. A. Clugston, PCID v.5.9, University of New South Wales, 2003.  
<sup>7</sup>P. T. Landsberg and G. S. Kousik, *J. Appl. Phys.* **56**, 1696 (1984).  
<sup>8</sup>L. J. Geerligs, G. P. Wyers, R. Jensen, O. Raaness, A. N. Waernes, S. Santen, A. Reinink, and B. Wiersma B, Energy Research Centre of the Netherlands Report No. ECN-RX-02-042 (2002).  
<sup>9</sup>R. A. Sinton, A. Cuevas, and M. Stuckings, Proceedings of the 25th IEEE Photovoltaic Specialists Conference, 1996 (unpublished), p. 457.  
<sup>10</sup>T. S. Horányi, T. Pavelka, and P. Tüttö, *Appl. Surf. Sci.* **63**, 306 (1993).  
<sup>11</sup>R. A. Smith, *Semiconductors* (Cambridge University Press, Cambridge, 1978); C. M. Wolfe, N. Holonyak, and G. E. Stillman, *Physical Properties of Semiconductors* (Prentice-Hall, Englewood Cliffs, 1989); P. Blood and J. W. Orton, *The Electrical Characterization of Semiconductors: Majority Carriers and Electron States* (Philips Research Laboratories, London, 1992).  
<sup>12</sup>A. Herguth, G. Schubert, M. Kaes, and G. Hahn, *Prog. Photovoltaics* **16**, 135 (2008).  
<sup>13</sup>N. D. Arora, J. R. Hauser, and D. J. Roulston, *IEEE Trans. Electron Devices* **ED-29**, 292 (1982).  
<sup>14</sup>L. M. Falicov and M. Cuevas, *Phys. Rev.* **164**, 1025 (1967).  
<sup>15</sup>N. Sclar, *Phys. Rev.* **104**, 1559 (1956).  
<sup>16</sup>D. A. Anderson and N. Apsley, *Semicond. Sci. Technol.* **1**, 187 (1986).  
<sup>17</sup>J. F. Lin, S. S. Li, L. C. Linares, and K. W. Teng, *Solid-State Electron.* **24**, 827 (1981).  
<sup>18</sup>P. Norton, T. Braggins, and H. Levinstein, *Phys. Rev. B* **8**, 5632 (1973).  
<sup>19</sup>O. Nichiporuk, A. Kaminski, M. Lemiti, A. Fave, and V. Skryshevsky, *Sol. Energy Mater. Sol. Cells* **86**, 517 (2005).  
<sup>20</sup>G. Coletti, L. J. Geerligs, P. Manshanden, C. Swanson, H. Habenicht, W. Warta, J. Arumughan, and R. Kopecek, Proceedings of the 22nd EU PVSEC, 2007 (unpublished), p. 989.  
<sup>21</sup>L. J. Geerligs and D. Macdonald, *Prog. Photovoltaics* **12**, 309 (2004).